Band alignment of $B_{0.14}Al_{0.86}N/Al_{0.7}Ga_{0.3}N$ heterojunction

Haiding Sun, Young Jae Park, Kuang-Hui Li, C. G. Torres Castanedo, Abdulmohsen Alowayed, Theeradetch Detchprohm, Russell D. Dupuis, and Xiaohang Li

Citation: Appl. Phys. Lett. **111**, 122106 (2017); doi: 10.1063/1.4999249
View online: http://dx.doi.org/10.1063/1.4999249
View Table of Contents: http://aip.scitation.org/toc/apl/111/12
Published by the American Institute of Physics

Band alignment of $B_{0.14}Al_{0.86}N/Al_{0.7}Ga_{0.3}N$ heterojunction

Haiding Sun,[1] Young Jae Park,[2] Kuang-Hui Li,[1] C. G. Torres Castanedo,[1] Abdulmohsen Alowayed,[1] Theeradetch Detchprohm,[2] Russell D. Dupuis,[2] and Xiaohang Li[1]
[1]*King Abdullah University of Science and Technology (KAUST), Advanced Semiconductor Laboratory, Thuwal 23955-6900, Saudi Arabia*
[2]*Center for Compound Semiconductors and School of Electrical and Computer Engineering, Georgia Institute of Technology, Atlanta, Georgia 30332, USA*

(Received 7 August 2017; accepted 9 September 2017; published online 21 September 2017)

Owing to large bandgaps of BAlN and AlGaN alloys, their heterojunctions have the potential to be used in deep ultraviolet and power electronic device applications. However, the band alignment of such junctions has not been identified. In this work, we investigated the band-offset parameters of a $B_{0.14}Al_{0.86}N/Al_{0.7}Ga_{0.3}N$ heterojunction grown by metalorganic vapor phase epitaxy. These specific compositions were chosen to ensure a sufficiently large band offset for deep ultraviolet and power electronic applications. High resolution transmission electron microscopy confirmed the high structural quality of the heterojunction with an abrupt interface and uniform element distribution. We employed high resolution X-ray photoemission spectroscopy to measure the core level binding energies of B 1s and Ga $2p_{3/2}$ with respect to the valence band maximum of $B_{0.14}Al_{0.86}N$ and $Al_{0.7}Ga_{0.3}N$ layers, respectively. Then, we measured the energy separation between the B 1s and Ga $2p_{3/2}$ core levels at the interface of the heterojunction. The valence band offset was determined to be 0.40 ± 0.05 eV. As a consequence, we identified a staggered-gap (type-II) heterojunction with the conduction band offset of 1.10 ± 0.05 eV. The determination of the band alignment of the $B_{0.14}Al_{0.86}N/Al_{0.7}Ga_{0.3}N$ heterojunction facilitates the design of optical and electronic devices based on such junctions. *Published by AIP Publishing*. [http://dx.doi.org/10.1063/1.4999249]

In the past few decades, conventional group-III-nitride materials, including GaN, AlN, and InN and their compound alloys, have been extensively studied because of their tunable bandgaps (from 0.6 to 6.2 eV) which have led to numerous optical and electronic device applications.[1–3] As an emerging member of the nitride family, wurtzite $B_xAl_{1-x}N$ ($0 \leq x \leq 1$) can also offer versatility for a tunable bandgap and lattice constant, making them promising materials for realizing ultraviolet (UV) and power devices.[4] In addition, Abid *et al*. have shown that BAlN layers with the increasing B-content could introduce strong refractive index contrast with respect to AlN and Al-rich AlGaN. Therefore, higher-B-content BAlN layers are expected to have a considerably lower refractive index which is a desirable feature for achieving high-reflectivity distributed Bragg reflectors (DBRs) operating in the deep-UV/UV range.[5] Furthermore, $B_xAl_{1-x}N$ alloys have lower lattice constants,[4] and thus, they can be used to tune the strain of epilayers via the formation of $B_xAl_{1-x}N$-based heterojunctions, such as in the form of BAl(Ga)N/Al(Ga)N. Recently, researchers have reported a significant increase in the UV spontaneous emission rate from BAl(Ga)N/AlGaN quantum well structures compared to the conventional AlGaN/AlGaN quantum well structures, which was attributed to the decrease in the built-in internal polarization fields through B incorporation.[6,7] Although previous studies have shown the potential applications of BAlN alloys, due to long-term difficulties in achieving single crystal wurtzite BAlN films with large B contents, the utilization of BAlN-based materials has been held back. Recently, we demonstrated thick single-phase wurtzite BAlN thin films ($\sim$100 nm) with boron (B) contents up to 14.4%.[8,9] This progress would enable further exploration of the feasibility of integrating BAlN films in the BAlN/AlGaN heterojunctions for various types of device applications.

The band offset of the BAlN/AlGaN heterojunction is a critical electronic parameter associated with designing semiconductor heterojunction devices because it determines the energy barriers for electron and hole transport, which is essential for the operation of such devices. The existing literatures have shown only band offset measurements of h-boron nitride (h-BN) with other semiconductor heterojunctions. For example, Majety *et al*. measured the band offsets of h-BN/6H-SiC heterojunctions and found that the conduction and valence band offset (VBO) values (ΔE_C and ΔE_V) of the h-BN/6H-SiC heterointerface were about 2.3 and 0.7 ($\pm$0.2) eV, respectively.[10] Liu *et al*. reported the band offset measurement of a wurtzite InN/h-BN heterojunction,[11] and King *et al*. presented the band offset at the BN/Si (100) interface[12] and the BN/Al_2O_3 interface[13] by using high resolution X-ray photoelectron spectroscopy (HR-XPS). However, a determining factor for the charge transport through the BAlN/AlGaN interface is the valence and conduction band alignment between BAlN and AlGaN layers. Until now, there has been a lack of experimental work on the band alignment parameters of the BAlN-related heterojunctions.

In this study, we carried out an HR-XPS study to determine the energy band alignment of a $B_{0.14}Al_{0.86}N/Al_{0.7}Ga_{0.3}N$ heterojunction by extrapolating the valence band offset (VBO) and the conduction band offset (CBO) at the interface. The compositions were selected to have a sufficiently large band offset for deep ultraviolet and power electronic applications. We also utilized high resolution transmission electron microscopy to investigate the $B_{0.14}Al_{0.86}N/Al_{0.7}Ga_{0.3}N$ interface quality including the compositional homogeneity. The band

alignment was presented, and the heterojunction type was identified.

The growth experiments of a 40 nm $B_{0.14}Al_{0.86}N$ layer on one *c*-plane AlN/sapphire template (sample A), a 400 nm $Al_{0.7}Ga_{0.3}N$ layer on another AlN/sapphire template (sample B), and a thin $B_{0.14}Al_{0.86}N$ (approximately 5 nm) layer on the 400 nm $Al_{0.7}Ga_{0.3}N$ layer on the third AlN/sapphire template (Sample C) were carried out by metalorganic vapor phase epitaxy (MOVPE). The *a* and *c* lattice constants of $B_{0.14}Al_{0.86}N$ and $Al_{0.7}Ga_{0.3}N$ are 3.027 and 4.798 (Ref. 4) and 3.135 and 5.047,[1] respectively. Thus, the in-plane lattice mismatch is 3.4%. The AlN template was grown similar to the previous report.[14] The schematics for Samples A-C are shown in Fig. 1. Triethylboron (TEB), trimethylaluminium (TMA), trimethylgallium (TMG), and NH_3 were used as precursors with H_2 being the carrier gas. The growth condition of the BAlN layer was the same as previously reported.[8] As the escape depth of photoemitted electrons in the HR-XPS is significantly low (5–10 nm), the overgrown $B_{0.14}Al_{0.86}N$ layer in the heterojunction sample had to be thin enough to collect the photoemission signal from both the $B_{0.14}Al_{0.86}N$ and $Al_{0.7}Ga_{0.3}N$ layers.

Subsequent to the growth, high-angle annular dark-field (HAADF) scanning transmission electron microscopy (STEM) measurements were performed using an FEI Probe-corrected Titan microscope which was operated at the acceleration voltage of 300 kV during the analysis. The compositional distribution of Al, B, and Ga elements in different layers was studied as well. This was accomplished by acquiring the energy-dispersive X-ray (EDX) spectroscopic spectra of Al and Ga elements and electron energy-loss spectroscopy (EELS) data for the light B element. The TEM specimens were prepared by using an FEI Helios dual-beam focused ion beam scanning electron microscope (DBFIB-SEM) system with a Ga ion source.

The core levels (CLs) and valence band photoemission spectra of $B_{0.14}Al_{0.86}N$ and $Al_{0.7}Ga_{0.3}N$ films were measured using the HR-XPS method which has been extensively utilized to measure the VBO of a heterointerface.[15–18] After the MOVPE growth, the samples were stored in the N_2 glove box of our MOVPE system. Due to the wafer transfer and cutting processes prior to the HR-XPS experiment, the samples were exposed to the air for about 20 min, which might have caused surface oxidation. No wafer cleaning was performed prior to the HR-XPS experiment.

The studies were carried out using a Kratos Axis Supra DLD spectrometer equipped with a monochromatic Al Kα X-ray source ($h\nu = 1486.6$ eV) operating at 150 W with a multi-channel plate and a delay line detector under a vacuum of $\sim 10^{-9}$ mbar. The spectra were recorded using an aperture slot of 110×110 μm^2. The high-resolution and survey spectra were collected at fixed analyzer pass energies of 20 and 160 eV, respectively. The samples were mounted in the floating mode to avoid differential charging, as charge neutralization was required for all these samples.[19] A low-energy electron flood gun (few eV) for the charge neutralization was utilized. The Kratos charge neutralization system allowed the low energy electrons to reach the sample from all directions as a result of their spiral trajectory. The sputtering process was not employed to reduce the surface oxide. Binding energies were referenced to the C 1s binding energy of adventitious carbon contamination, which was taken to be 284.8 eV.[18] The peak deconvolution was accomplished using the CasaXPS software.[15] For the CL spectra, experimental data points were fitted by the Voigt curve after the application of a linear background,[15] while the valence band maximum (VBM) energy in the spectrum was determined by extrapolating a linear fit of the leading edge of the valence band photoemission to the baseline.

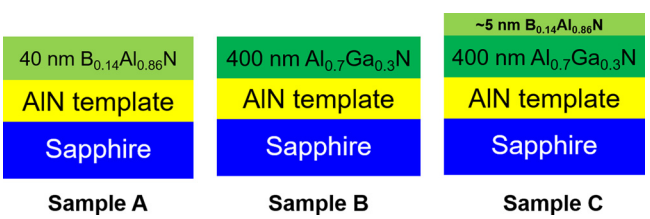

FIG. 1. Schematics of the three investigated samples.

The HAADF-STEM image in Fig. 2(a) shows an abrupt interface between the $B_{0.14}Al_{0.86}N$ layer and the $Al_{0.7}Ga_{0.3}N$ layer. Figure 2(b) presents the elemental distribution from the EDX scan of Al and Ga and the EELS scan of B across the interface, confirming a uniform distribution of the elements in the grown epilayers. B is a light atom, which cannot be resolved by EDX, and thus, EELS was utilized to detect the B element. Due to the relatively high Al content in the $B_{0.14}Al_{0.86}N$ layer as compared to the $Al_{0.7}Ga_{0.3}N$ layer, we observed a brighter red color in the upper part of the Al map. Furthermore, both Fast Fourier Transform (FFT) patterns of the $B_{0.14}Al_{0.86}N$ and $Al_{0.7}Ga_{0.3}N$ layer show a single-phase wurtzite structure, as can be seen in Fig. 2(c).

To evaluate the VBO at the $B_{0.14}Al_{0.86}N/Al_{0.7}Ga_{0.3}N$ interface, the CLs of B 1s and Ga 2p were used in the analysis.[12,15] The VBO of the $B_{0.14}Al_{0.86}N/Al_{0.7}Ga_{0.3}N$ heterojunction can be determined using Eq. (1) derived by using the method explained by Kraut *et al.*[20]

$$\Delta E_v = \left(E_{B1s}^{BAlN} - E_{VBM}^{BAlN}\right) - \left(E_{Ga2p3/2}^{AlGaN} - E_{VBM}^{AlGaN}\right) + \left(E_{Ga2p3/2}^{BAlN/AlGaN} - E_{B1s}^{BAlN/AlGaN}\right). \quad (1)$$

The first term on the right side of the equation is the CL energy of B 1 s determined with respect to the VBM of sample A.

Figure 3(a) shows the B 1s CL spectrum collected from the $B_{0.14}Al_{0.86}N$ layer, which was deconvoluted using two peaks. The peak observed at 190.4 eV corresponds to B in the $B_{0.14}Al_{0.86}N$ layer, while the peak located at 191.8 eV was likely due to the oxidized B complex.[21] The origin of the surface oxidation could come from the XPS sample preparation process before loading the sample into the chamber. Figure 3(b) depicts the valence band spectrum where the VBM of the sample was obtained by linearly extrapolating the leading edge to the baseline of the respective valence band photoelectron spectrum. The VBM of the $B_{0.14}Al_{0.86}N$ was measured to be 2.3 eV. Thereby, the separation between the CL energies of B 1s and VBM [$\Delta E = (E_{B1s}^{BAlN} - E_{VBM}^{BAlN})$] for $B_{0.14}Al_{0.86}N$ is 188.1 eV.

To calculate the term in the second brackets in Eq. (1), the XPS spectrum of Sample B was measured. We observed

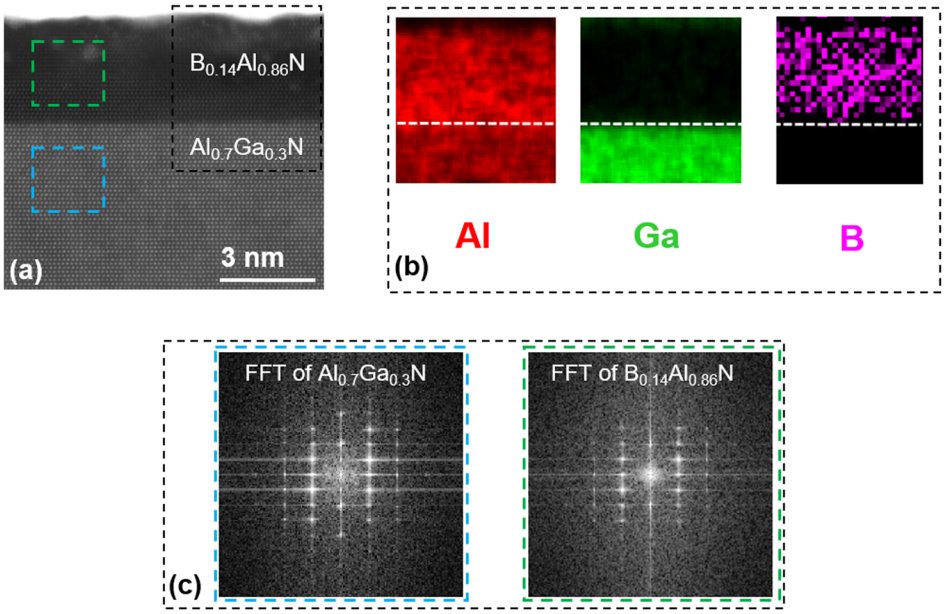

FIG. 2. (a). A cross-sectional HAADF-STEM [11-20] image of sample B at the heterojunction interface. (b) The EDX element map of Al and Ga and the EELS element map of B from the black dashed area in (a). The white dashed line marks the interface. (c) The fast Fourier transform (FFT) patterns from the blue and green boxes of the $Al_{0.7}Ga_{0.3}N$ and $B_{0.14}Al_{0.86}N$ layer in (a), respectively.

that the CL of Ga $2p_{3/2}$ is located at 1117.3 eV from the $Al_{0.7}Ga_{0.3}N$ layer [Fig. 4(a)], while the VBM was measured to be 2.6 eV [Fig. 4(b)]. Thereby, the separation between the CL energy of Ga $2p_{3/2}$ and the VBM $[\Delta E = (E^{AlGaN}_{Ga2p} - E^{AlGaN}_{VBM})]$ for the $Al_{0.7}Ga_{0.3}N$ layer was determined to be 1114.7 eV. A small shoulder with a peak energy of 1118.7 eV (not shown here) existed on the left side of the major peak in the Ga 2p3/2 spectra, which indicates a slightly surface oxidation of the AlGaN film (sample B). The origin of the surface oxidation could be from the HR-XPS sample preparation process as well.

The last term in Eq. (1) represents the CL separation between the B 1s and Ga $2p_{3/2}$ peaks, which was measured from the XPS spectrum of sample C. Figures 5(a) and 5(b) show the B 1s and Ga 2p CLs which originated from sample B, respectively. Figure 5(a) demonstrates that the deconvoluted B 1s CL spectrum showed the B 1s chemical state at 190.3 eV. The Ga $2p_{3/2}$ CL was located at 1117.3 eV [Fig. 5(b)]. Thus, the energy difference between the CLs of Ga $2p_{3/2}$ and B 1s $[\Delta E = (E^{BAlN/AlGaN}_{Ga2p} - E^{BAlN/AlGaN}_{B1s})]$ was calculated to be 927.0 eV.

Thus, the VBO can be determined using Eq. (2) from which we obtained $\Delta Ev = 0.4 \pm 0.05$ eV. More detailed experiments to rule out differential charging were not performed, but based on the prior works by DiStefano and Bersch *et al.*, the magnitude of any differential charging is expected to be within the error of the measurements.[13,22]

Thereby, by substituting the VBO (ΔE_v) and the electronic bandgap values of $B_{0.14}Al_{0.86}N$ ($E_g = 5.7$ eV)[4] and $Al_{0.7}Ga_{0.3}N$ ($E_g = 5.0$ eV)[22] in Eq. (2), we can measure the CBO (ΔE_c) for the $B_{0.14}Al_{0.86}N/Al_{0.7}Ga_{0.3}N$ heterostructure.

$$\Delta E_c = \left(E_g^{BAlN} + \Delta E_v - E_g^{AlGaN}\right). \quad (2)$$

Hence, based on Eq. (2), the resultant CBO (i.e., ΔE_c) is 1.1 $\pm$ 0.05 eV. Inevitably, there was tensile strain in the $B_{0.14}Al_{0.86}N$ epilayer due to the heteroepitaxial growth. However, studies have shown that the effect of strain on both CBO and VBO was almost negligible by comparing the strained and unstrain heterojunctions, generally less than 0.1 eV.[23,24]

The experimentally determined parameters from this study were incorporated into a band alignment diagram as shown in Fig. 6. The figure suggests that the band alignment of the $B_{0.14}Al_{0.86}N/Al_{0.7}Ga_{0.3}N$ heterostructure is a type-II heterostructure. This unique bandgap alignment between $B_{0.14}Al_{0.86}N$ and $Al_{0.7}Ga_{0.3}N$ could aid the development of III-nitride light emitters. For instance, the UV-transparent BAlN layer could be employed as an electron blocking layer as a result of the large CBO for AlGaN-based emitters.

By using the band alignment of InN, GaN, and AlN at room temperature reported by Van de Walle and Neugebauer[23,25] and Roul *et al.*,[26] we also plotted the band alignment of $B_{0.14}Al_{0.86}N/Al_{0.7}Ga_{0.3}N$ along with InN, GaN,

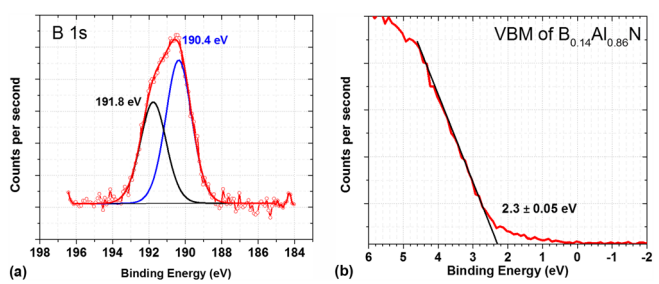

FIG. 3. (a) CL of B 1s and (b) valence band spectra of the $B_{0.14}Al_{0.86}N$ layer (sample A).

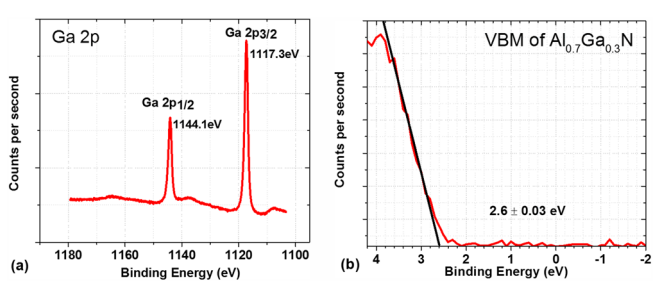

FIG. 4. (a) CL of Ga 2p and (b) valence band spectra of the $Al_{0.7}Ga_{0.3}N$ layer (sample B).

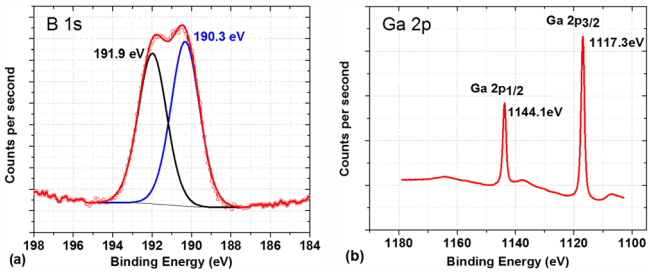

FIG. 5. (a) CLs of B 1 s and (b) Ga 2p spectra of the $B_{0.14}Al_{0.86}N/Al_{0.7}Ga_{0.3}N$ heterojunction (sample C).

and AlN in Fig. 6, showing that the value of ΔE_c is larger in the $B_{0.14}Al_{0.86}N/Al_{0.7}Ga_{0.3}N$ heterojunction compared to the AlN/GaN heterojunction. The VBO of AlN/GaN is 1.12 eV,[28] and the VBO of InN/GaN is the one reported by King *et al.*, showing a valence band offset of 0.58 eV.[16] Based on the diagram, we obtain the CBOs of BAlN/AlN, BAlN/GaN, and BAlN/InN of 0.5, 2.4, and 4.8 eV, respectively. Also, we can extract the VBOs of BAlN/AlN, BAlN/GaN, and BAlN/InN heterojunctions of 0.9, 0.1, and 0.9 eV, respectively. Therefore, the type-II, II, and I heterojunctions can be formed in BAlN/AlN, BAlN/GaN, and BAlN/InN heterojunctions, respectively. The BAlN layer would offer the largest CBO to provide a larger electron confinement and blocking effect. These characteristics could offer numerous degrees of freedom and provide further guidance for designing nitride devices by incorporating the BAlN layers.

For example, BAlN can be potentially applied in GaN-based electronics by replacing Al(Ga)N as the barrier layer. Studies have shown that the power density and total power available from GaN-based high electron mobility transistors (HEMTs) are superior to those of the Si- and GaAs-based transistors by using GaN as the channel for two-dimensional electron gas (2DEG).[29] In this study, we calculated the 2DEG sheet carrier concentration n_s for both AlN/GaN and $B_{0.14}Al_{0.86}N$/GaN heterojunctions using the below equation[30]

$$n_s = \frac{\sigma\left[\frac{(B)AlN}{GaN}\right]}{e} - \left[\frac{\epsilon_0\epsilon[(B)AlN]}{d_{(B)AlN}e^2}\right] \times \left[e\emptyset_b + E_f - \Delta E_C\right]. \quad (3)$$

$\frac{\sigma\left[\frac{(B)AlN}{GaN}\right]}{e}$ is the calculated piezoelectric and spontaneous polarization induced sheet charge density (total bond sheet charge), e is the electron charge, $\epsilon[(B)AlN]$ is the relative dielectric constant of (B)AlN, ϵ_0 is the vacuum permittivity, $d_{(B)AlN}$ is the thickness of the (B)AlN deposited on top of the GaN layer, $e\emptyset_b$ is the Schottky barrier height, E_f is the Fermi level of GaN at the interface of (B)AlN/GaN at room temperature, and ΔE_C is the CBO of (B)AlN and GaN heterojunctions. The other parameters including the lattice, spontaneous polarization, piezoelectric, and dielectric constants of AlN, GaN, and BN can be referred from the study by Ambacher *et al.*[1] We used Vegard's law assuming no bowing to obtain the parameters for $B_{0.14}Al_{0.86}N$ alloys and assumed that both the AlN layer and the $B_{0.14}Al_{0.86}N$ layer have a thickness of 10 nm. Therefore, the 2DEG sheet carrier concentrations from Eq. (3) were 5.88×10^{13} and $7.37 \times 10^{13}\,cm^{-2}$ for the AlN/GaN and $B_{0.14}Al_{0.86}N$/GaN heterojunctions, respectively, indicating an approximately 25% increase in the sheet carrier concentration by adopting the $B_{0.14}Al_{0.86}N$/GaN heterojunction. Thus, BAlN is potential for GaN-based electronics.

In summary, we have grown single-phase $B_{0.14}Al_{0.86}N$ and $Al_{0.7}Ga_{0.3}N$ layers and their heterojunction with an abrupt interface on AlN/sapphire templates by MOVPE. The determination of the band offset parameters in the $B_{0.14}Al_{0.86}N/Al_{0.7}Ga_{0.3}N$ heterostructure was carried out using the HR-XPS. We determined the VBO and CBO to be 0.4 eV and 1.1 eV, respectively, with a type-II band heterostructure alignment. We also plotted the band alignment of the $B_{0.14}Al_{0.86}N/Al_{0.7}Ga_{0.3}N$ heterojunction along with the conventional binary nitrides (AlN, GaN, and InN), which could provide valuable support in the design of BAlN-based heterostructures. As an example, we calculated the 2DEG sheet carrier concentration in the $B_{0.14}Al_{0.86}N$/GaN heterojunction and showed its potential in electronic devices by comparing with a typical AlGaN/GaN-based heterostructure.

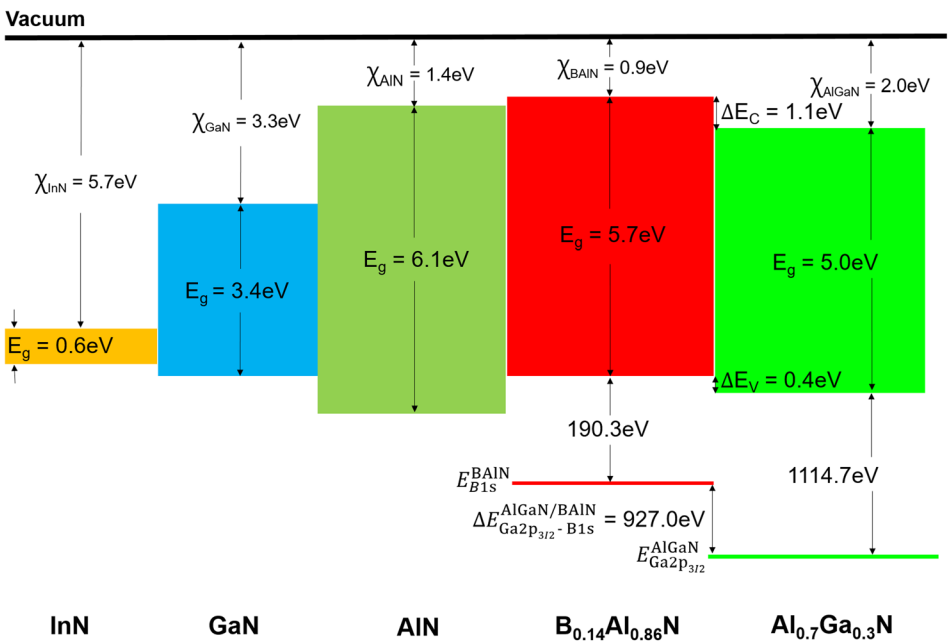

FIG. 6. Schematic diagram of the band alignment diagram in the $B_{0.14}Al_{0.86}N/Al_{0.7}Ga_{0.3}N$ heterojunction, along with the band edge alignment between AlN and InN (Refs. 25–27).

The KAUST authors would like to acknowledge the support of GCC Research Program No. REP/1/3189-01-01, Baseline No. BAS/1/1664-01-01, and Equipment No. BAS/1/1664-01-07. The work at Georgia Institute of Technology was supported in part by DARPA under Grant No. W911NF-15-1-0026 and NSF under Grant No. DMR-1410874. R.D.D. acknowledges the additional support of the Steve W. Chaddick Endowed Chair in Electro-Optics and Georgia Research Alliance.

[1]O. Ambacher, B. Foutz, J. Smart, J. R. Shealy, N. G. Weimann, K. Chu, M. Murphy, A. J. Sierakowski, W. J. Schaff, L. F. Eastman, R. Dimitrov, A. Mitchell, and M. Stutzmann, J. Appl. Phys. **87**, 334 (2000).
[2]B. Janjua, H. Sun, C. Zhao, D. H. Anjum, F. Wu, A. A. Alhamoud, X. Li, A. M. Albadri, A. Y. Alyamani, M. M. El-Desouki, T. K. Ng, and B. S. Ooi, Nanoscale **9**, 7805 (2017).
[3]F. Wu, H. Sun, I. A. Ajia, I. S. Roqan, D. Zhang, J. Dai, C. Chen, Z. C. Feng, and X. Li, J. Phys. D: Appl. Phys. **50**, 245101 (2017).
[4]M. Zhang and X. Li, Phys. Status Solidi B **254**, 1600749 (2017).
[5]M. Abid, T. Moudakir, G. Orsal, S. Gautier, A. E. Naciri, Z. Djebbour, J.-H. Ryou, G. Patriarche, L. Largeau, H. J. Kim, Z. Lochner, K. Pantzas, D. Alamarguy, F. Jomard, R. D. Dupuis, J.-P. Salvestrini, P. L. Voss, and A. Ougazzaden, Appl. Phys. Lett. **100**, 051101 (2012).
[6]S.-H. Park and D. Ahn, IEEE Photonics Technol. Lett. **28**, 2153 (2016).
[7]S.-H. Park, Opt. Express **23**, 3623 (2015).
[8]X. Li, S. Wang, H. Liu, F. A. Ponce, T. Detchprohm, and R. D. Dupuis, Phys. Status Solidi B **254**, 1600699 (2017).
[9]S. Wang, X. Li, A. M. Fischer, T. Detchprohm, R. D. Dupuis, and F. A. Ponce, J. Cryst. Growth **475**, 334 (2017).
[10]S. Majety, J. Li, W. P. Zhao, B. Huang, S. H. Wei, J. Y. Lin, and H. X. Jiang, Appl. Phys. Lett. **102**, 213505 (2013).
[11]J. Liu, X. Liu, X. Xu, J. Wang, C. Li, H. Wei, S. Yang, Q. Zhu, Y. Fan, X. Zhang, and Z. Wang, Nanoscale Res. Lett. **5**, 1340 (2010).
[12]S. King, M. French, J. Bielefeld, M. Jaehnig, M. Kuhn, G. Xu, and B. French, Appl. Phys. Lett. **101**, 42903 (2012).
[13]J. Distefano, Y. C. Lin, J. Robinson, N. R. Glavin, A. A. Voevodin, J. Brockman, M. Kuhn, B. French, and S. W. King, J. Electron. Mater. **45**, 983 (2016).
[14]X. Li, S. Wang, Y. O. Wei, H. Xie, T. T. Kao, M. Satter, S. C. Shen, P. D. Yoder, T. Detchprohm, R. D. Dupuis, A. Fischer, and F. A. Ponce, Phys. Status Solidi B **252**, 1089–1095 (2015).
[15]M. Tangi, P. Mishra, C. Tseng, T. K. Ng, M. N. H. D. H. Anjum, M. S. Alias, N. Wei, L. Li, and B. S. Ooi, ACS Appl. Mater. Interfaces **9**, 9110 (2017).
[16]P. D. C. King, T. D. Veal, C. E. Kendrick, L. R. Bailey, S. M. Durbin, and C. F. McConville, Phys. Rev. B **78**, 033308 (2008).
[17]M. Akazawa, T. Matsuyama, T. Hashizume, M. Hiroki, S. Yamahata, and N. Shigekawa, Appl. Phys. Lett. **96**, 132104 (2010).
[18]T. L. Duan, J. S. Pan, and D. S. Ang, Appl. Phys. Lett. **102**, 201604 (2013).
[19]Y. Mori, M. Tanemura, and S. Tanemura, Appl. Surf. Sci. **228**, 292 (2004).
[20]E. A. Kraut, R. W. Grant, J. R. Waldrop, and S. P. Kowalczyk, Phys. Rev. Lett. **44**, 1620 (1980).
[21]W. E. Moddeman, A. R. Burke, W. C. Bowling, and D. S. Foose, Surf. Interface Anal. **14**, 224 (1989).
[22]E. Bersch, M. Di, S. Consiglio, R. D. Clark, G. J. Leusink, and A. C. Diebold, J. Appl. Phys. **107**, 043702 (2010).
[23]C. G. Van de Walle and J. Neugebauer, Appl. Phys. Lett. **70**, 2577 (1997).
[24]S. Wei and A. Zunger, Appl. Phys. Lett. **69**, 2719 (1996).
[25]C. G. Van de Walle and J. Neugebauer, Nature **423**, 626 (2003).
[26]B. Roul, M. Kumar, M. K. Rajpalke, T. N. Bhat, and S. B. Krupanidhi, J. Phys. D: Appl. Phys. **48**, 423001 (2015).
[27]H. X. Jiang and J. Y. Lin, Semicond. Sci. Tech. **29**, 84003 (2014).
[28]S. Vitanov, "Simulation of high electron mobility transistors," Ph.D. dissertation (TU Wien, Austria, 2010).
[29]U. K. Mishra, P. Parikh, and Y. Wu, Proc. IEEE **90**, 1022 (2002).
[30]I. P. Smorchkova, L. Chen, T. Mates, L. Shen, S. Heikman, B. Moran, S. Keller, S. P. DenBaars, J. S. Speck, and U. K. Mishra, J. Appl. Phys. **90**, 5196 (2001).